Supporting Information

Facile Synthesis of Vanadium-Modulated CoFeP@C Nanoparticles to Enhanced Intrinsic Activity and Stability for High-Performance Oxygen Evolution Reaction

Yaoxia Yang*, Bolin Xiong, Dangxia Wang, Zhen Yao, Wei Zeng, and Dongfei Sun

Key Laboratory of Eco-functional Polymer Materials of the Ministry of Education,

Key Laboratory of Polymer Materials of Gansu Province, College of Chemistry and

Chemical Engineering, Northwest Normal University, Lanzhou 730070, China

*Corresponding author. College of Chemistry and Chemical Engineering, Northwest Normal University, Lanzhou, 730070.

E-mail address: yangyaoxia2007@126.com; yaoxiayang@nwnu.edu.cn.

1. Structure characterizations

The natural structural characteristics of the as-prepared samples are analyzed with following related instruments. The morphological characteristics and microstructure of samples were characterized by using field-emission scanning electron microscopy (FE-SEM, Carl Zeiss Ultra Plus, Germany) and transmission electron microscopy (TEM, JEOL JEM-2100, Tokyo, Japan), respectively. The surface specific chemical bond composition and crystal phase of samples were investigated with X-ray photoelectron spectrometer (XPS, Thermo Scientific K-Alpha) equipped a Al Kα radiation source and an X-ray powder diffraction (XRD, Rigaku D/Max-2400) using a Cu Kα radiation source. Fourier transform infrared (FT-IR) spectra were tested with a Digilab FTS-3000 Fourier by Bromatum kalium pellets method. First, the samples were degassed in 120 °C vacuum for 12 h, then the pore-size distributions and surface areas of the as-prepared samples were investigate by the Brunauer-Emmett-Teller (BET) instrument. The specific chemical composition and distribution of the catalysts were characterized via energy-dispersive X-ray spectroscopy (EDS, Oxford, England) equipped with an Aztec-X-80.

2. Electrochemical measurements

All electrochemical measurements were performed in a standard three-electrode system at an electrochemical workstation (CHI760e, CH Instruments, Shanghai, China) with a 5 mm diameter GCE as the working electrode, a graphite rod as the counter electrode, and Hg/HgO electrode as the reference electrodes. The working electrode is prepared as described below: To prepare the catalyst ink, 5 mg of each catalysts were

dispersed in a mixture solution of 20 μL of Nafion solution (5 wt%) and 480 μL of ethanol with the assistance of ultrasonication for 90 min. 10 μL of ink was then dropped onto a clean glassy carbon electrode (GCE) with a diameter of 5 mm using a pipette, and dried at room temperature (catalyst loading~0.51 mg cm^{-2}). The aqueous solutions of 1.0 M KOH was used as the electrolyte for all processes in the electrochemical test. All the potentials were converted into the reversible hydrogen electrode (vs. RHE) by the Nernst equation:

$$E\ (RHE) = E\ (Hg/HgO) + 0.059\ pH + 0.098$$

The experiments were all performed at room temperature. The OER performance was evaluated in N_2-saturated 1.0 M KOH, the linear sweep voltammetry (LSV) with a scan rate of 5 mV s^{-1}. Tafel plots were measured in linear portion through concrete calculation via Tafel equation: $\eta = a + b \log j$ (where η, b, j represent the overpotential, the Tafel slope and the current density, respectively). The double-layer capacitance (C_{dl}) of the catalysts were calculated from cyclic voltammetry (CV) at different scan rates within a small potential range (0.979-1.079 V vs. RHE for OER) where no Faradaic redox reactions occur. The electrochemical impedance spectroscopy (EIS) measurements were conducted with a frequency range from 10^{-2} Hz to 10^{-6} Hz and EIS spectra were fitted by the ZView software. We tested the stability of the catalyst in the OER by testing the GCE loaded with the best sample for 1000 cycles of CV at a scan rate of 20 mV s^{-1}, and the electrochemical durability tests were examined by chronopotentiometry curves at the current densities of 10 mA cm^{-2} for 20 h. In addition, no iR compensation was performed on the test data.

3. Turnover frequency (TOF) calculation

TOF of catalyst was calculated using a method used in the literature, e.g. ACS. Catal. 2018, 8, 1683-1689. It was calculated with the following equation:

$$\mathrm{TOF} = \frac{|J| \cdot A}{4F \cdot n}$$

Where $|J|$ (A cm^{-2}) represents the current density at a fixed voltage during the LSV measurement, A is the geometric area of the working glassy carbon electrode (0.02 cm^2), F is the Faraday constant (96485 C mol^{-1}), and n is the number of active sites (mol). The factor of 4 is the corresponding electron transfer numbers of OER.

The number of active sites (n) was calculated by using the methods in previously reported paper. Firstly, the catalyst was examined employing cyclic voltammogram in 1.0 M PBS solution with the constant potential range of -0.2 to 0.6 V (vs. RHE) at a scan rate of 500 mV s^{-1}. The number of active sites n is proportional to the charge Q, which can be calculated from the obtained CV curve by integrating. Therefore, active sites could be obtained from the following equation:

$$\mathrm{n} = \frac{Q}{2F} = \frac{I \cdot t}{2F} = \frac{I \cdot V/u}{2F} = \frac{S}{2F \cdot u}$$

Where S is integrated effective area in CV recorded, I is the current density (A), V is the voltage (V), u is the scan rate (500 mV s^{-1}).

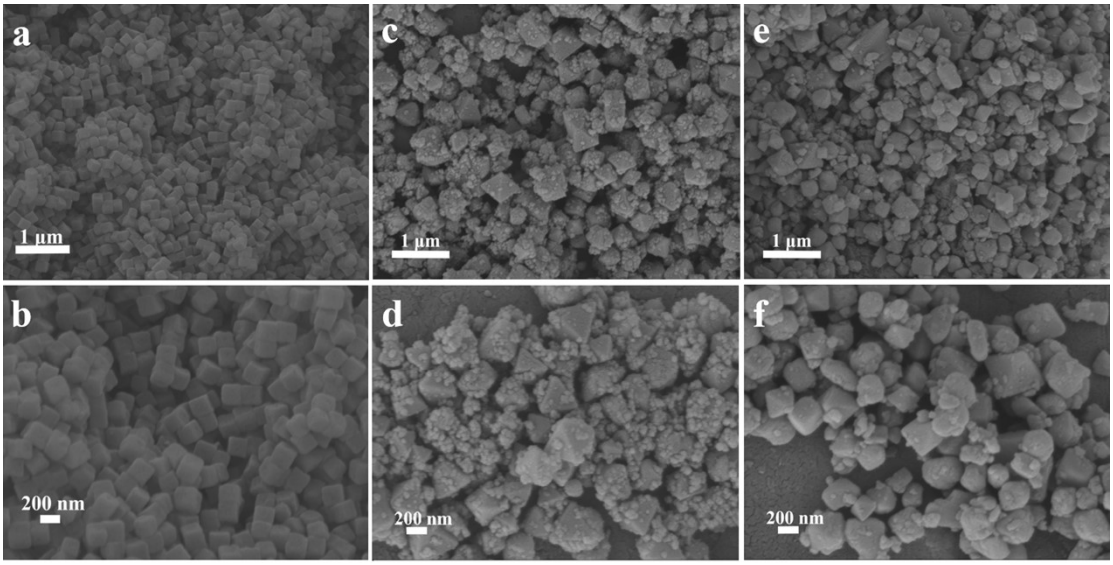

Fig. S1 SEM images of (a, b) CoFe PBA, (c, d) CoFe PBA@C, (e, f) V-CoFe PBA@C at different magnifications.

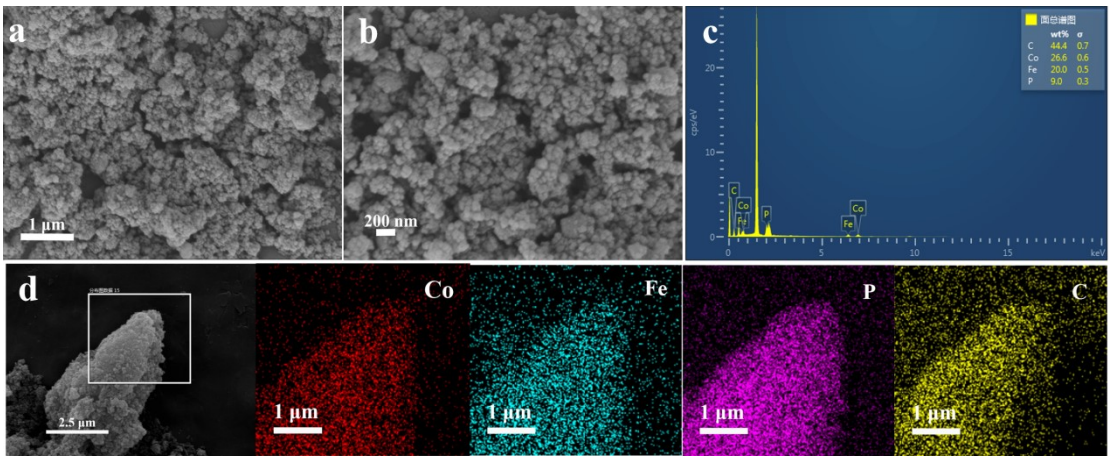

Fig. S2 (a, b) SEM images at different magnifications, (c) The EDS elemental analysis, (d) SEM image and elemental mapping of CoFeP@C.

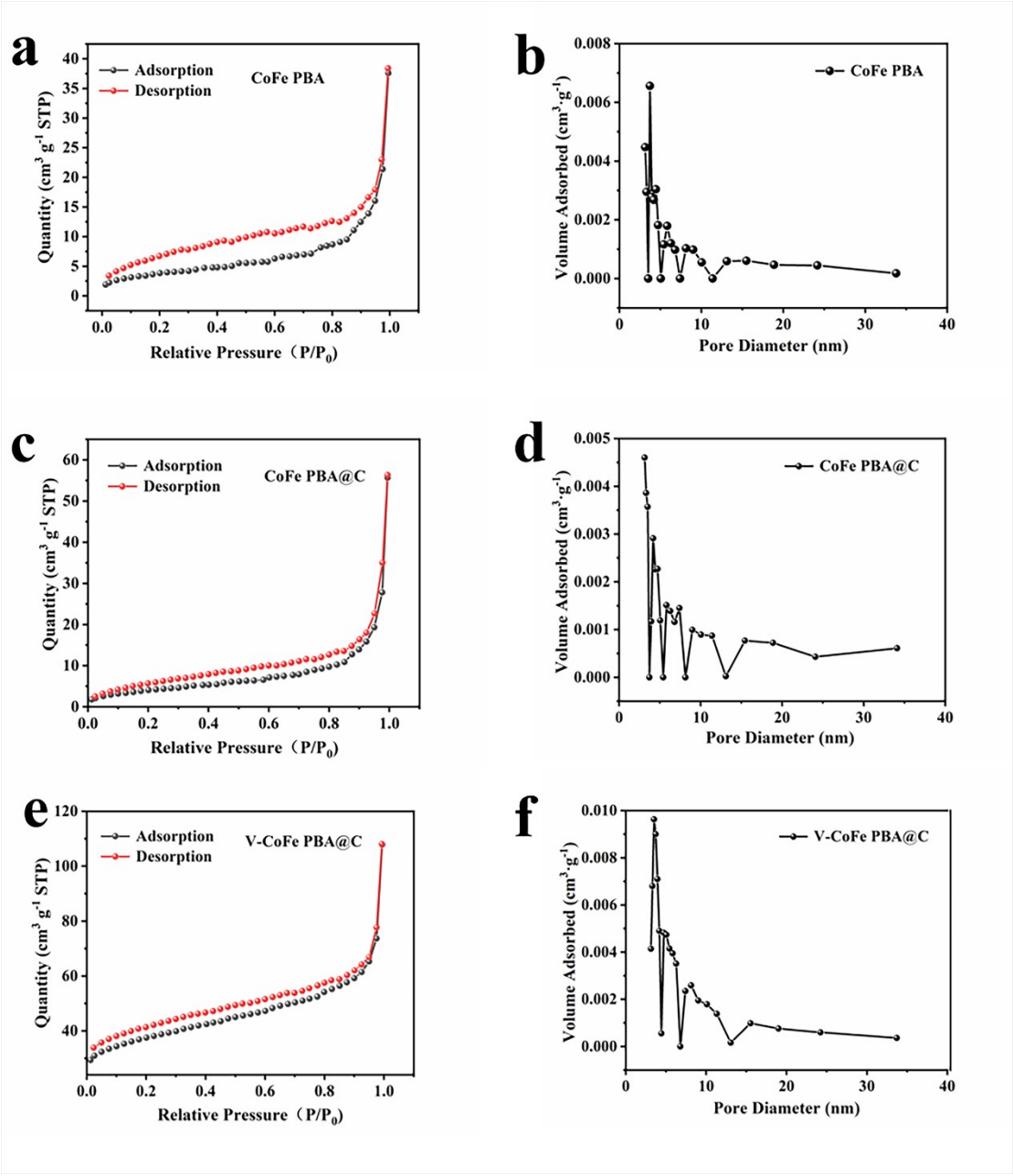

Fig. S3 N_2 adsorption/desorption isotherms and pore-size distributions of (a, b) CoFe PBA, (c, d) CoFe PBA@C, (e, f) V-CoFe PBA@C.

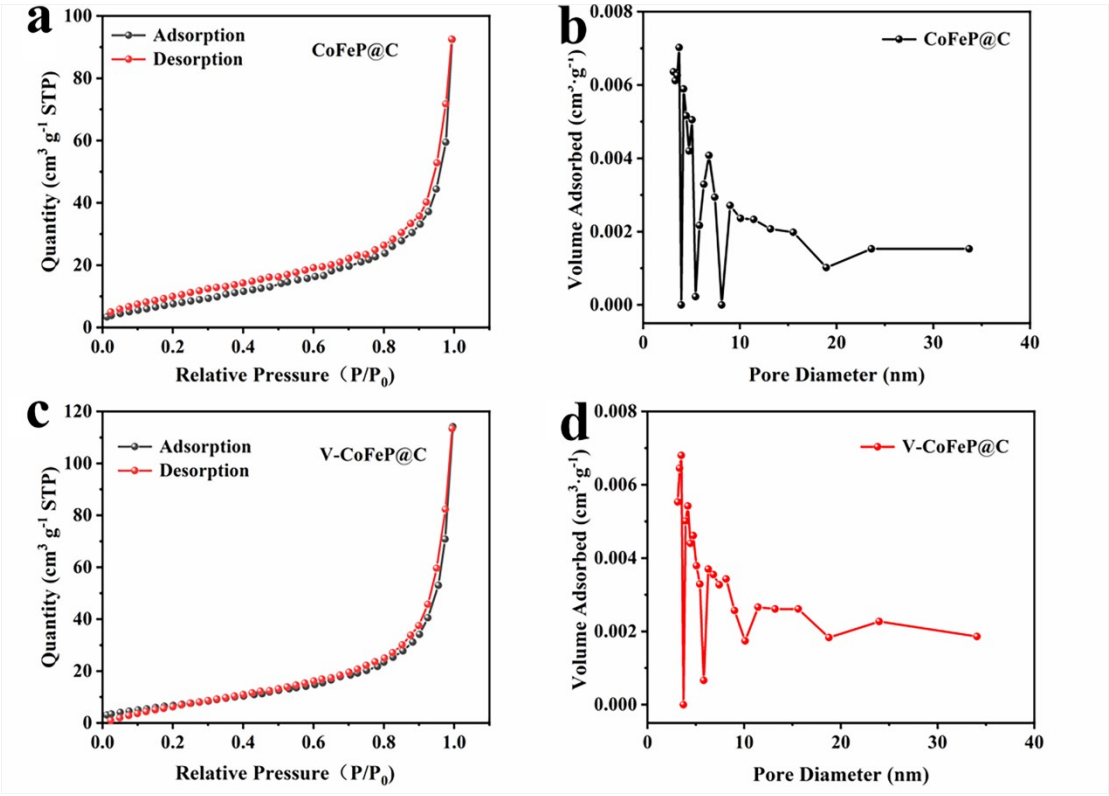

Fig. S4 N_2 adsorption/desorption isotherms and pore-size distributions of (a, b) CoFeP@C, (c, d) V-CoFeP@C.

Table S1 BET surface area and pore volume of the samples

Catalyst	**BET surface area** $[m^2\ g^{-1}]$	**Pore volume** $[cm^3\ g^{-1}]$
CoFe PBA	11.309	0.053
CoFe PBA@C	12.770	0.083
V-CoFe PBA@C	24.676	0.108
CoFeP@C	29.012	0.137
V-CoFeP@C	33.047	0.178

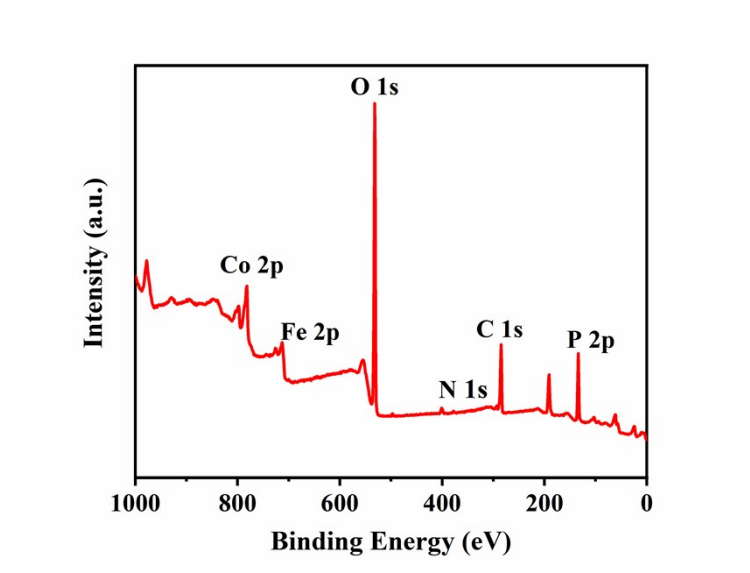

Fig. S5 XPS survey spectrum of V-CoFeP@C.

Table S2 OER parameters of various as-prepared catalysts in 1 M KOH

Catalyst	η_{10} (mV)	Tafel slope (mV dec^{-1})	C_{dl} (mF cm^{-2})	R_{ct} (Ω)
CoFe PBA	372	93.15	1.90	152.6
CoFe PBA@C	353	80.52	5.10	95.98
V-CoFe PBA@C	319	69.77	10.30	43.04
CoFeP@C	293	61.37	19.10	21.27
V-CoFeP@C	265	57.15	23.80	5.00

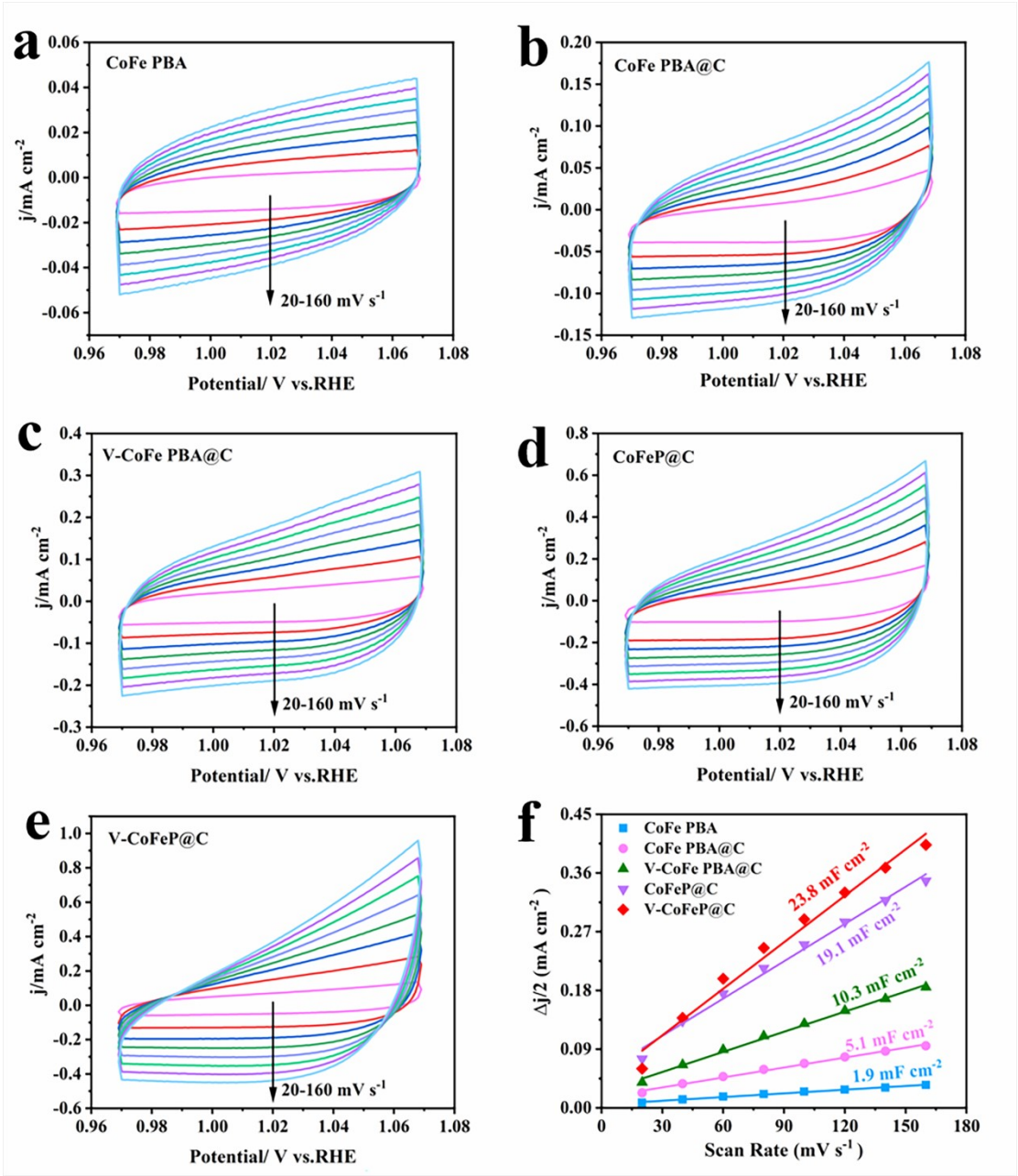

Fig. S6 (a, b, c, d, e) CV curves of the CoFe PBA, CoFe PBA@C, V-CoFe PBA@C, CoFeP@C and V-CoFeP@C at different scan rate of 20, 40, 60, 80, 100, 120, 140 and 160 $mV \cdot s^{-1}$, (f) C_{dl} values of as-prepared samples.

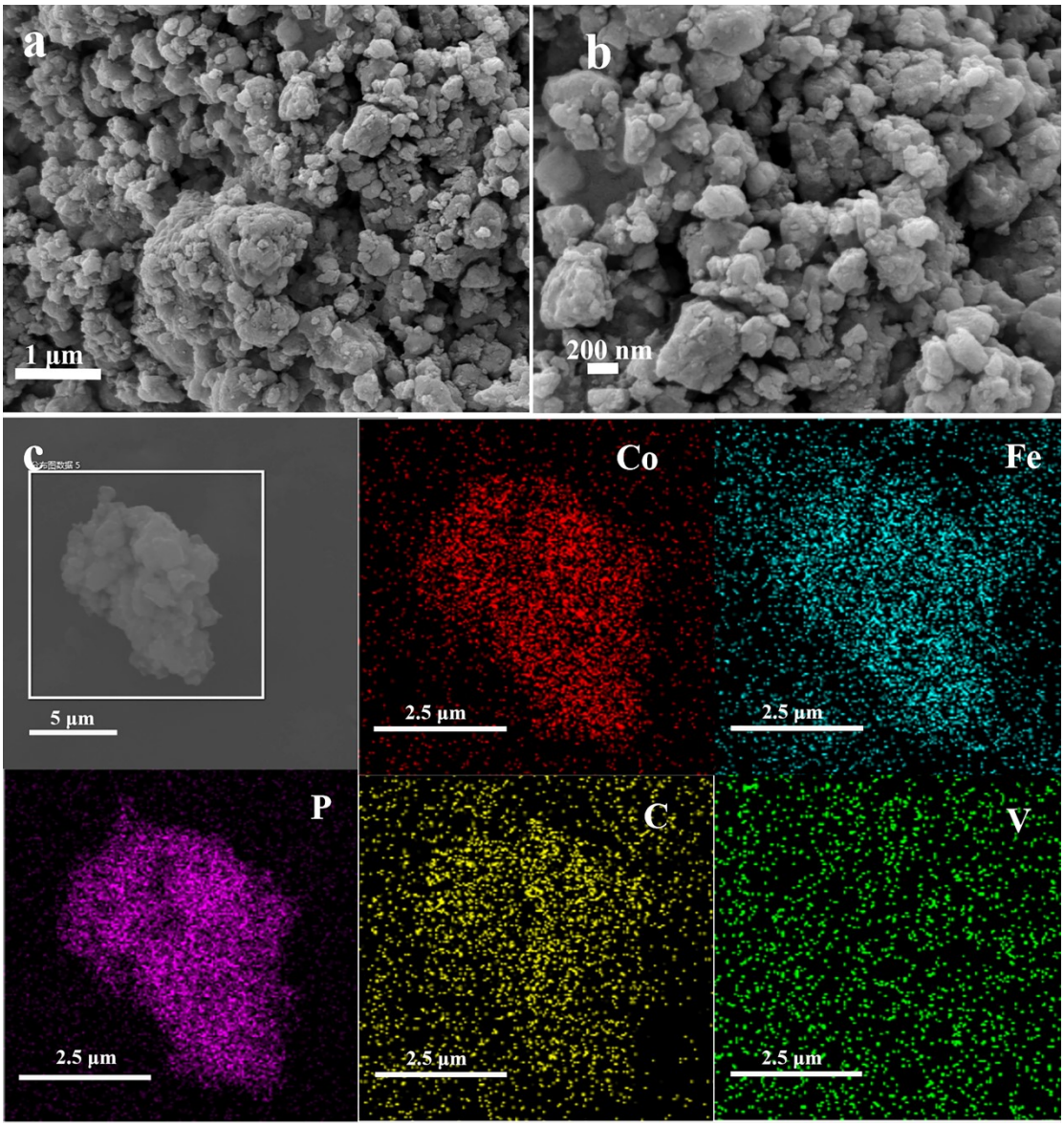

Fig. S7 (a, b) SEM images and (c) the corresponding element mappings of V-CoFeP@C after CP long-term stability test OER in 1 M KOH.

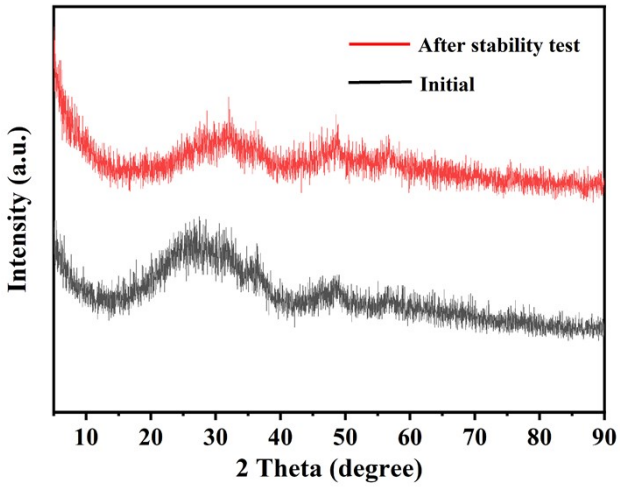

Fig. S8 XRD patterns of pristine V-CoFeP@C before and after CP long-term stability test OER in 1 M KOH.

Table S3 Comparison of OER performance of V-CoFeP@C with other advanced reported electrocatalysts in 1.0 M KOH.

Catalyst	η_{10} (mV)	Ref.
$Co_{2.0}Fe_{0.5}Cr_{0.5}$	203	[S1]
V-Co_9S_8/CoO/NC	231	[S2]
CoO/Co_3O_4@NC	263	[S3]
V-CoFeP@C	265	This work
CoSi-Fe	289	[S4]
NiCoFe-P	290	[S5]
Co@Ni-MOF	293	[S6]
Ni-$FeSO_4$rGO-STNF	308	[S7]
CoP CNFs	325	[S8]
Co-VN@C	330	[S9]
bi-CoPc carbon	357	[S10]
Co/VN@NC	440	[S11]

References

[S1] Chavan H S, Patil D R, Yoo J E, Kim J, Choi Y, Lee S, Lee K. Enhanced oxygen evolution reaction activity and stability through Fe and Cr Co-incorporation in cobalt hydroxide. J. Electroanalytical Chem., **2025**, 992: 119249.

[S2] Airam S, Shaheen M, Sulaman M, Rehman K, Gao J, Yang L, Naim A F A, Murtaza G, Ahmad N. Revealing the potential of vanadium doped Co_9S_8/CoO/NC electrocatalyst triggering HER and OER for alkaline water splitting. J. Alloy Compd., **2025**, 1033: 181209.

[S3] Zhang K, Li N N, Weng Y L, Kang Y B, Lee J Y, Zhang H F, Ding Y H, Han X T, Pang H. Navigating covalency of cobalt oxides for enhanced oxygen evolution. Adv. Funct. Mater., **2025**, 2507212.

[S4] Tan X F, Ding C T, Wang Y, Chen D Z, Liang T, Meng C G, Zhang Y F. Modulating electronic structure of cobalt silicate by iron-doping ensuring the boosted oxygen evolution reaction properties. J. Colloid Interf. Sci., **2025**, 699: 138168.

[S5] Yang L Q, Li L. Synthesis of uniformly dispersed NiCoFe trimetallic phosphide for efficient overall water splitting. J. Phys. Chem. Solids, **2025**, 207: 112926.

[S6] Sivakumar M, Vediyappan V, Bhuvaneshwari M, Muthukutty B, Kumar P S, Kim S C, Alagumalai K, Sandoval H G. Sphere-like Co-doped Ni metal-organic framework for enhanced oxygen evolution reaction. J. Phys. Chem. Solids, **2025**, 207: 112918.

[S7] Amani E. Fetohi, Dena Z Khater, R S Amin, K M El-Khatib. Nickel sulfide–

transition metal sulfides bi-electrocatalyst supported on nickel foam for water splitting. J. Phys. Chem. Solids, 2025, 207: 112906.

[S8] Xie X Q, Liu J P, Gu C N, Li J J, Zhao Y, Liu C S. Hierarchical structured CoP nanosheets/carbon nanofibers bifunctional eletrocatalyst for high-efficient overall water splitting. J. Energy Chem., 2021, 64: 503-510.

[S9] Peng T, Guo Y, Zhang Y G, Wang Y B, Zhang D Y, Yang, Y, Lu Y, Liu X F, Chu P K, Luo Y S. Uniform cobalt nanoparticles-decorated biscuit-like VN nanosheets by in situ segregation for Li-ion batteries and oxygen evolution reaction. Appl. Surf. Sci., 2021, 536: 147982.

[S10] Huang Q E, Chen J, Luan P, Ding C M, Li C. Understanding the factors governing the water oxidation reaction pathway of mononuclear and binuclear cobalt phthalocyanine catalysts. Chem. Sci., **2022**, 13: 8797-8803.

[S11] Zhao X M, Han Q L, Li J D, Du X H, Liu G H, Wang Y J, Wu L L, Chen Z W. Ordered macroporous design of sacrificial Co/VN nano-heterojunction as bifunctional oxygen electrocatalyst for rechargeable zinc-air batteries. Chem. Eng. J., **2022**, 433: 133509.